Comparison of Different Machining Strategies and Their Effects on CNC Vertical Machining Center

CNC Dik İşleme Merkezi Tezgahında Farklı İşleme Stratejileri ve Etkilerinin Karşılaştırılması

Ömer Faruk Öztürk

Marmara University, Faculty of Technology, Department of Mechanical Engineering, Istanbul, Türkiye

Kürşat Tanrıver*

Assist. Prof., Istanbul Health and Technology University, Faculty of Engineering and Natural Sciences, Department of mechatronics Engineering, Istanbul, Türkiye

Mustafa Ay

Prof. Dr., Marmara University, Faculty of Technology, Department of Mechanical Engineering, Istanbul, Türkiye

** Corresponding author: kursat.tanriver@istun.edu.tr*

Geliş Tarihi / Received: 25.03.2024
Kabul Tarihi / Accepted: 16.06.2024
Araştırma Makalesi/Research Article
DOI: 10.5281/zenodo.13855946

ABSTRACT

In today's world, interest in the aviation sector and developments within it continue to grow at an accelerated pace. With this increase, the demand for the production of components for unmanned aerial vehicles, passenger airplanes, or jet aircraft has risen correspondingly. However, due to the complex structure of aviation parts, the strategy employed during their processing is of significant importance. The distortion issue encountered in the machining of aviation parts, particularly in thin-walled components, leads to unwanted dimensional changes and significantly complicates the production of these parts.

This study aims to investigate the effects of different machining techniques on the widely used Al 7075 T7351 aluminum alloy in the aviation sector and to contribute the experimental results to both readers and the literature. In the experiments, samples of Al 7075 T7351 aluminum alloy with thicknesses of 1.00 mm, 1.20 mm, and 1.50 mm were processed using various machining strategies. According to the experimental results, the effect of tool strategy on thickness was observed to vary between a minimum of 0.67% and a maximum of 7.78%. Taking the average of the minimum and maximum values of the three samples, the average effect of the tool path strategy on surface roughness was found to be 55.46%, and its effect on parallelism varied between 37.50% and 112.50%.

Furthermore, it is believed that the methods presented in this study will contribute to solving similar problems in other industries, in addition to the aviation sector, in areas such as material selection, determination of processing parameters, and compliance of three-dimensional coordinate measurements (CMM) with standards.

Keywords: Aluminum alloys, Distortion control, Thin-walled parts, Machining parameters, CMM

ÖZET

Günümüzde havacılık sektörüne olan ilgi ve gelişmeler artarak devam etmektedir. Bu artışla beraber insansız hava araçları, yolcu uçakları veya jet uçaklarının komponent üretimine olan talep o oranda artmaktadır. Ancak havacılık parçalarının karmaşık yapıda olmaları sebebiyle işlenme sırasındaki strateji oldukça önemlidir. Havacılık parçalarının işlenmesinde karşılaşılan distorsiyon sorunu, özellikle ince cidarlı bileşenlerde istenmeyen boyutsal değişimlere neden olmakta ve bu parçaların üretiminde önemli ölçüde zorluk oluşturmaktadır.

Bu çalışma ile havacılık sektöründe çokça kullanılan Al 7075 T7351 alüminyum alaşımının farklı işleme teknikleri üzerindeki etkileri araştırılarak deney sonuçlarının okuyucuya ve literatüre katkı sunulması amaçlanmıştır. Deneylerde 1,00 mm, 1,20 mm ve 1,50 mm kalınlıklarındaki üç farklı Al 7075 T7351 alüminyum alaşım malzeme örnekleri çeşitli işleme stratejileri kullanılarak işlenmiştir. Deney sonuçlarına göre takım stratejisinin kalınlığa etkisi en fazla %7,78 ve en az %0,67 oranında olduğu görülmüştür. Üç numunenin minimum ve maksimum değerlerinin ortalaması alındığında takım yolu stratejisinin yüzey pürüzlülüğü üzerindeki ortalama etki değeri %55,46 ve paralelliğe etkisi ise %37,50 ile % 112,50 oranında değişiklik gösterdiği görülmüştür.

Ayrıca bu çalışmada sunulan yöntemler, malzeme seçimi, işleme parametrelerinin belirlenmesi ve üç boyutlu koordinat ölçümlerinin (CMM) standartlara uygunluğu gibi konularda, havacılık sektörünün yanında diğer endüstrilerde benzer sorunların çözümüne katkıda bulunacağı düşünülmektedir.

Anahtar Kelimeler: Alüminyum alaşımları, Distorsiyon kontrolü, İnce cidarlı parçalar, İşleme parametreleri, CMM

1. INTRODUCTION

CNC milling, one of the most common and efficient processes in modern manufacturing, involves removing excess material from the surface of a workpiece intermittently with a rotating tool to achieve geometric shape and dimensional accuracy that meet technical requirements (Zhou et al., 2023). However, it should be recognized that various challenges arise during machining, necessitating efforts to address them effectively. It is understood that identifying the right machining strategies can contribute to longer tool life, lower machining costs, reduced scrap costs, and the attainment of more precise surfaces (Sato et al., 2023).

Geometric dimensioning and tolerancing emerge from the need to define the functionality and geometric technical specifications of an industrial product, which are verified through dimensional measurements using various devices. One of these measurement techniques is coordinate measurement. The development of coordinate measurement techniques was observed in the early 1970s, where coordinate measuring devices were initially limitedly used in laboratories (Işık, 2019). Today, as product geometries become more complex, three-dimensional coordinate measuring machines (CMMs) have become one of the most critical components of modern manufacturing technology (Trapet et al., 2004; Aggogeri et al., 2011; Vlaeyen et al., 2023). By directly integrating CMMs into modern production, they play a significant role in the inspection stages of these production systems. Coordinate measuring machines are devices capable of measuring dimensions, shapes, and positional deviations with high accuracy within the same system. The precision of the part to be produced, the quantity of parts, and the measurement uncertainty are important criteria in the choice of a measurement system (Weckenmann, 2011). CMMs are commonly used in precision measurement applications and play a crucial role in evaluating profile errors (Le et al., 2024). The automated operation and reporting capabilities of CMM machines minimize delays caused by external factors and maximize efficiency (Zhu, 2010). Distortion in parts measured by devices like CMMs is defined as the deviation of part dimensions from their original dimensions after the part is removed from the fixture. Distortion typically occurs due to factors such as the material type, residual stresses in the material, residual stresses resulting from CNC machining, and part design. Among these factors, the most significant is the residual stresses in the material's internal structure originating from the manufacturing process. These residual stresses arise from production and shaping processes such as quenching, forging, extrusion, casting, welding, and machining. Specific strategies, as addressed in this article, can minimize these distortions caused by machining processes.

A literature review was conducted for coordinate measuring machines (CMMs), which are widely adopted in acceptance and re-verification processes (Lee et al., 2022; Yang et al., 2022). Some of these studies are as follows. Lin et al. (2023) designed a perforated plate and performed measurements. Kim et al. (2023) focused on flatness, Franco & Jodar (2021) on horizontal, and Pahk & Kim (1995) on ring size measurements. Pahk & Burdekin (1991) measured a horizontal plane by observing the probe tip position to determine parametric rotation and linearity errors. Sudatham et al. (2015) used an optical scanned pulsed interferometer to measure parametric positioning errors. Umetsu et al. (2005) developed a new laser tracking system to measure parametric errors from axes. Ballu et al. (2006) proposed a new design approach recommending initiating the three-dimensional modeling of the product at the design stage to define functional features and design parameters as soon as possible. Anselmetti (2006) developed a semi-automatic system that creates a functional specification based on the interface between components. This system automatically generates data frames on parts and provides information on contacting elements. Hu & Peng (2011) developed a computer-aided tolerance system based on axiomatic design for functional design. They determined the main stages for axiomatic design. The first is the creation of a rule-based technical diagram and the allocation of values to each tolerance. In the second stage, they considered manufacturing and cost-related effects. Cao et al. (2013) first defined the main part and basic features, then described a method that adds functionality with assembly analysis. They then proposed an iterative flow procedure to generate data on other individual parts. Göhler et al. (2016) proposed a methodological framework that turns functional requirements into design parameters. In this framework, besides geometry, other different parameters such as material and external factors were considered. They established a connection between the desired tolerance and functionality. Rouetbi et al. (2017) developed a methodology for the functional tolerance of a hyperstatic mechanical system. This methodology first evaluates assembly as rigid. In the second step, it defines the deformation capacity to ensure the assembly of the system. Anselmetti et al. (2005) and Royer & Anselmetti (2016) provided a perspective on the selection of manufacturing to fit the functional features defined by the designer. This perspective can be used to describe the situation between manufacturing characteristics and subsequent manufacturing stages. Göktaş et al. (2017) created a toolpath using the offsetting method in their study. Toolpath data obtained from software and applications were tested on suitable billet parts on CNC machines. The experiments resulted in no machining errors due to residue and gaps.

This study aims to share the results of processing Al 7075 T7351 Aluminum alloy material using different techniques, providing advance information to readers who will process this material and thus filling the gap in the literature. For this purpose, three different thicknesses of Al 7075 T7351 series aluminum alloy material, namely 1.00 mm, 1.20 mm, and 1.50 mm, were processed in experiments. The distortion problem encountered in the processing of aviation parts, especially causing undesired dimensional variations in thin-walled components, emerges as a significant problem in the industry. This study contributes to the literature by presenting how different processing strategies affect this distortion problem and which strategies are more applicable. Additionally, the methods presented in this study, such as material selection, determination of processing parameters, and compliance of CMM measurements with standards, are considered applicable in solving similar problems in the aviation and other industries. In this context, the aim is to provide useful information for solving industrial problems and to contribute to the solution of production processes in sensitive industries such as the aviation sector.

2. MATERIAL and METHOD

Due to the complex nature of aviation components, processing them can be quite challenging. Particularly, during the machining of thin-walled parts, distortion can occur, leading to variations in the desired dimensions of the parts. In this study, three designed thin-walled sample parts were processed using different machining strategies, aiming to determine which method is more feasible based on the results obtained from them.

Material

To observe distortion changes and prepare experimental samples, Al 7075 T7351 series aluminum alloy billets were procured. The chemical properties of the AL 7075 series material are presented in Table 1 (Pandian & Kannan, 2022). This material has various hardening conditions, such as T6, T651, T73, T7351, and T76 (Khalid et al., 2023). In this study, Al 7075 T7351 series aluminum alloy material was preferred due to its low density, superior tensile strength, excellent corrosion resistance (Imran & Khan, 2019), and frequent use in the aviation sector.

Table 1. Chemical composition of 7075 Aluminum Alloy (Pandian & Kannan, 2022).

Chemical composition	Al	Zn	Mg	Cu	Fe	Mn	Cr	Si	Ti	Other
Content (wt %)	89.3	5.3	2.5	1.6	0.5	0.3	0.23	0.4	0.2	0.15

Due to material costs, it was decided to prepare three experimental specimens at model scale, with raw material dimensions set at 90 mm x 60 mm x 30 mm. Before preparing the test specimens, the entire design was modeled in the Catia V5 program. In order to observe distortion and enable comparison, three thin-walled parts of different thicknesses were designed. The thicknesses of the parts were chosen as 1.00 mm, 1.2 mm, and 1.5 mm, respectively. The dimensions of the test specimens are shown in Figure 1a, and the untreated state of the billet is shown in Figure 1b.

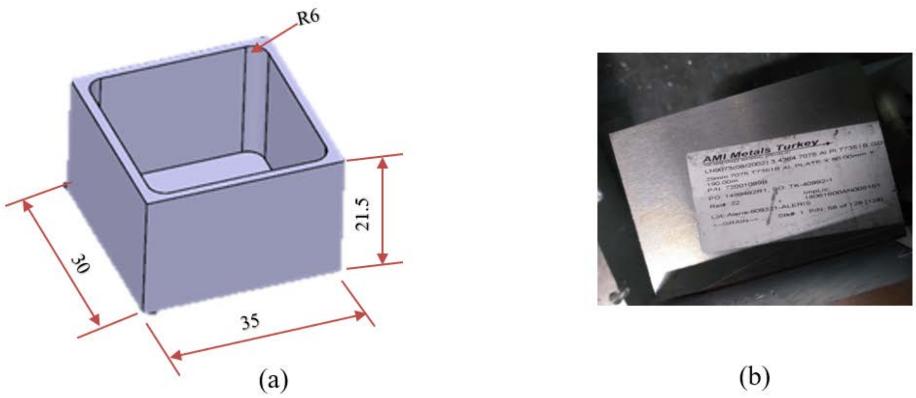

(a) (b)

Figure 1. The experimental specimen (a) the solid model (b) the AL 7075 T7351 series aluminum alloy material

In order to achieve the desired precision, it is essential to appropriately determine the process parameters of the selected machining method and ensure that the part is securely fixed to prevent any movement or deformation (Gameros et al., 2017). For the purposes of this study, a fixture was designed to facilitate access along the z-axis of the CNC machine and to aid in machining. Additionally, it was observed that this elevation and fixture design is necessary for ensuring the accuracy of dimensions, form precision, and surface quality of the finished workpiece (Poyraz & Yandı, 2021). Furthermore, it is expected that the use of the fixture will contribute to productivity, tool life, reduced machine movement, and consequently, shorter machining times (Snigdha et al., 2017). The elevation and fixture design are illustrated in Figure 2, where the elevation is shown in gray and the fixture in purple. Three 10.5 mm diameter pilot holes were drilled for securing the fixture and workpiece, followed by tapping M12x1.5 threaded holes into these pilot holes. The Allen head bolts used for fastening are of 8.8 quality, 60 mm in length, and fully threaded according to DIN 933 standards. The bolts were tightened with preload and torque according to DIN 13.

(a) (b)

Figure 2. Elevation and fixture design (a) solid model (b) real model

Long tool life, achieving the desired surface quality, and minimizing chip formation during machining are facilitated by the tool holder shown in Figure 3a, known as short thick Shrink holders (Bozdemir et al., 2023). Carbide end milling cutters suitable for processing Al 7075 material have been selected (Arslan et al., 2024). For roughing operations, a four-fluted finger mill with a diameter of D16, as shown in Figure 3b, has been used. For finishing operations, a three-fluted finger mill with a diameter of D8, as illustrated in Figure 3c, has been employed.

(a) (b) (c)

Figure 3. Tool holder and cutting tools selection (a) Shrink (b) D8 three-flute end mill (c) D16 four-flute end mill

Method

As production processes accelerate and advance, the necessity for swiftly making acceptance or rejection decisions for produced parts increases. To meet this need, Coordinate Measuring Machines (CMMs) are widely utilized in both manufacturing and quality control domains. Just as rapid measurements are crucial, swift decision-making is equally important for part machining strategy, and standardized rules exist for these evaluations. In this study, the EN ISO 14253-2 standard was referenced for thickness and surface roughness measurements. However, although the EN ISO 14253-2 standard focuses on uncertainty calculations in dimensional measurements, it does not cover coordinate measurements (Balsamo, 2023; Maltauro, et al., 2023; Maltauro et al., 2024). In this work, a CMM device was used for coordinate measurements. The standards outlining the calculation methods for CMM measurements are the ISO 15530 Series (Shaheen et al., 2023; Wojtyła et al., 2023), and ISO 10360-2 (ISO 10360-2, 2009). The uncertainty measurement, verification, and calibration of the utilized device were conducted in accordance with these standards (Cauchick-Miguel et al., 1996).

In this article, a three-axis CNC milling machine was employed for machining processes, while the CAM module of the widely used (Jamaludin et al., 2023) Catia V5 software was utilized for Computer-Aided Manufacturing (CAM) applications. This enabled the device to perform measurements and machining according to CAM simulation by selecting different tooling during the process. Subsequently, to investigate how the samples would perform under different stresses, they were connected to the CNC machine, and machining operations were performed to remove chips. The milling process is illustrated in Figure 4. Measurements were conducted using a CMM.

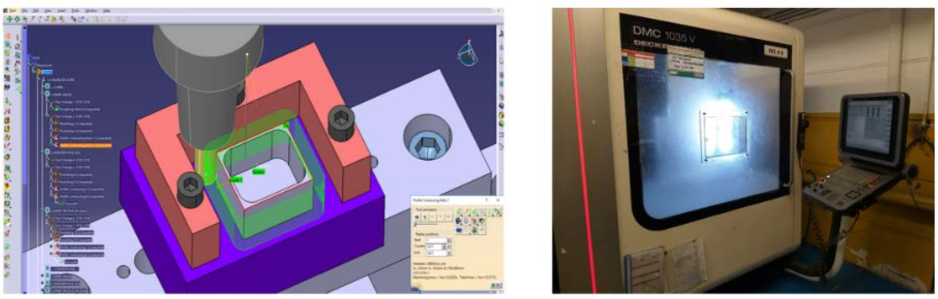

(a) (b)

Figure 4. Milling operation (a) CAM processing (b) CNC vertical machining

For the experiment, machining was performed on three different parts named Sample 1, Sample 2, and Sample 3, each with the same external dimensions but different thicknesses. The experiment samples consist of three pieces of Al 7075 T7351 series aluminum alloy material, each fixed with three zinc-plated M12 bolts, with thicknesses of 1.00, 1.20, and 1.50 mm. For the milling process, rough chip removal operation was performed on the part initially to clear the pool remaining inside the part. Following this process, finishing operations were attempted to obtain final dimensions by machining the inner walls using three different toolpath machining strategies: helix, zig, and zig-zag. In helix machining, a toolpath was created by moving around the part without interrupting its contact with the part simultaneously in all three axes. In zig toolpath strategy, cutting was done in one direction, entering the part from the same direction after each pass. In zig-zag strategy, after the tool exits the part from one direction, it enters the next pass from the direction it exited. The cutting tool performed cutting operation in both directions. For these operations, the spindle speed was calculated as 8400 rpm, feed rate as 5000 mm/min, and the depth of cut was set as 1 mm. Simulation of the CAM program allows for easy detection of incidents such as tool holder and tool plunging into the part, or any other events that may cause damage during machining. The simulation image of rough chip removal operation is provided in Figure 5.

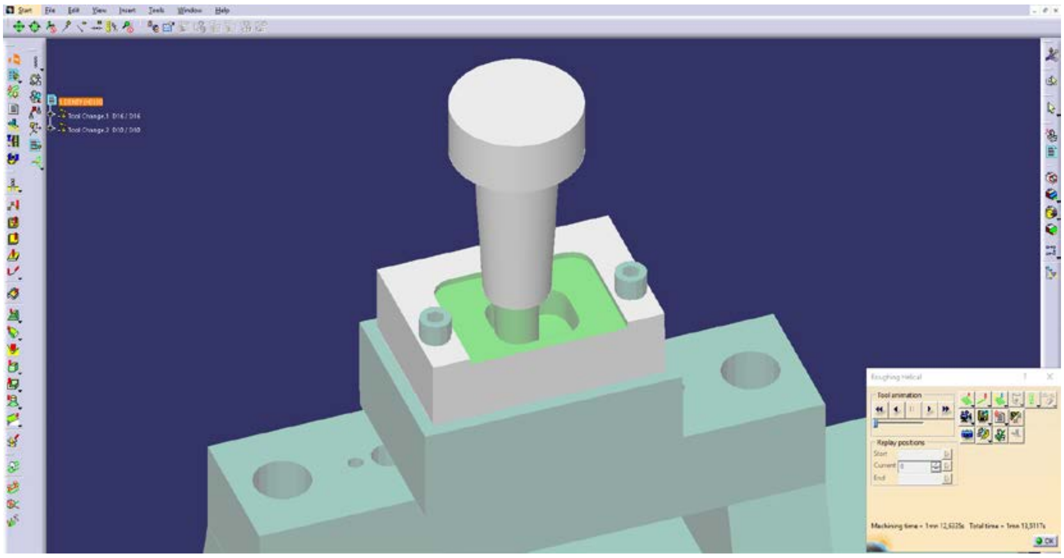

Figure 5. CAM simulation and analysis

3. RESULT and DISCUSSION

As a result of the machining process, measurements were taken for part thickness, surface roughness, and coordinate (CMM) dimensions, and shared in graphical form. Measurement result graphs for part thickness are provided for 1.00 mm in Figure 6a, 1.20 mm in Figure 6b, and 1.50 mm in Figure 6c. Accordingly, for the 1.00 mm thick part, a better result was obtained with a value of 0.97 mm using the helix-straight machining method. For the 1.20 mm thick part, a better result was obtained with a value of 1.21 mm using the helix-reverse machining method. For the 1.50 mm thick part, a better result was obtained with a value of 1.50 mm using the helix-reverse machining method. Additionally, when the averages of the machining strategies were evaluated in all three graphs, it can be observed that the dimensions obtained using the straight machining method are closer to the desired level compared to the reverse machining method.

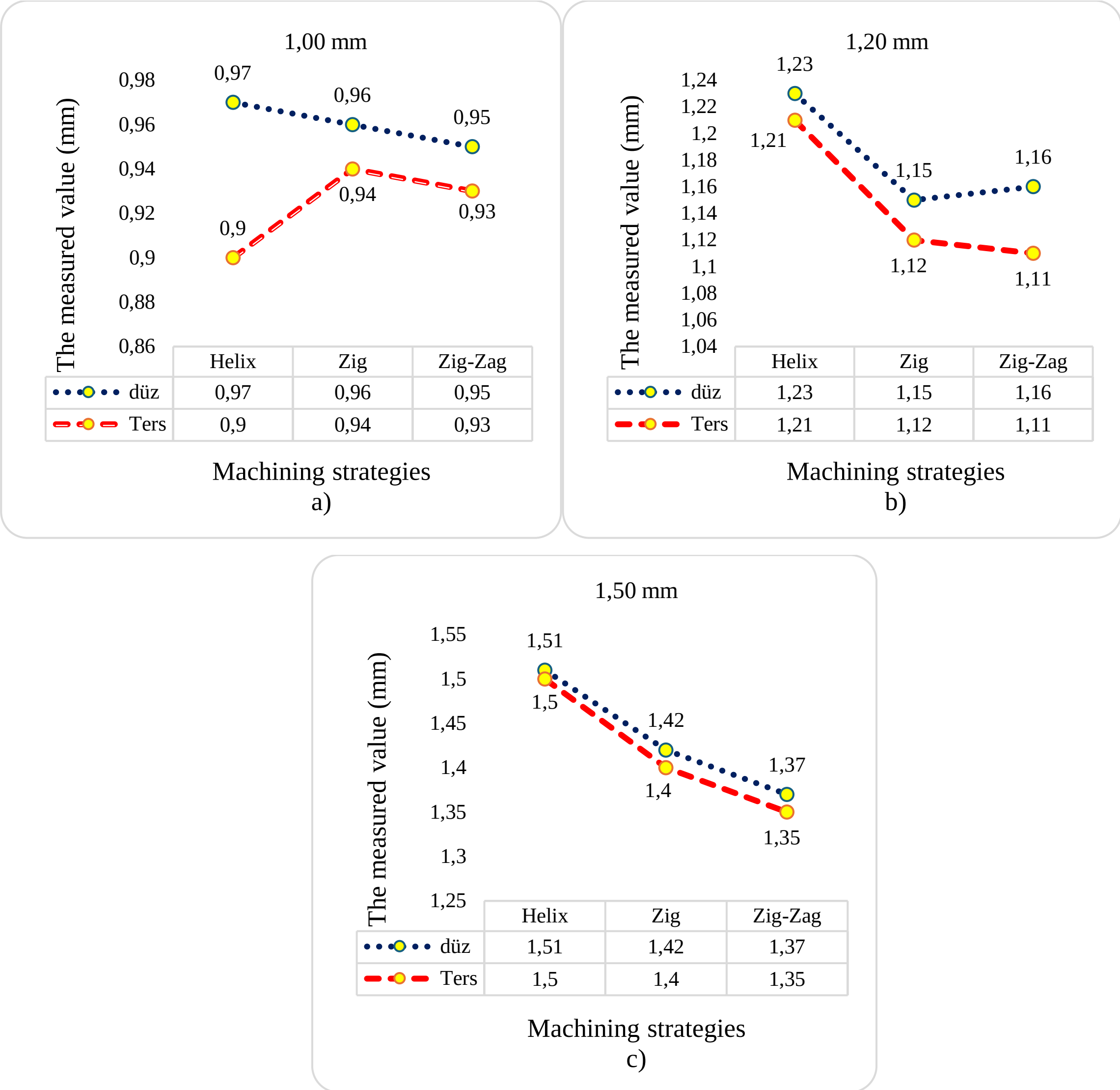

Figure 6. Thickness measurement (a) 1.00 mm (b) 1.20 mm (c) 1.50 mm

Here, when considering the maximum and minimum values in the three experimental samples, it has been evaluated that the tool machining strategy's effect on thickness ranges from a maximum of 7.78% to a minimum of 0.67%. In the study conducted by Motorcu & Bilge (2018), it was found that the cutting tool material alone had an influence of over 90% on dimensional integrity. Although the statistically significant effect of the other selected end milling parameters could not be determined, when considering the maximum and minimum values, the effect value on dimensional integrity was evaluated to be 3.70%.

Measurement results for part roughness are provided in Figure 7a for 1.00 mm thickness, Figure 7b for 1.20 mm thickness, and Figure 7c for 1.50 mm thickness. The surface roughness measurements were conducted in accordance with the TS EN 10049: 2014 standard. Accordingly, the best result for the 1.00 mm thick part was obtained with a reverse helix machining method, showing a value of 0.136 µm. For the 1.20 mm thick part, the best result was achieved with a straight zig machining method, indicating a value of 0.142 µm. The best result for the 1.50 mm thick part was found with a reverse helix machining, presenting a value of 0.108 µm. Moreover, when averaging the results of the machining strategies across all three graphs, it is observed that the reverse machining method results in a lower level of roughness compared to the straight machining method.

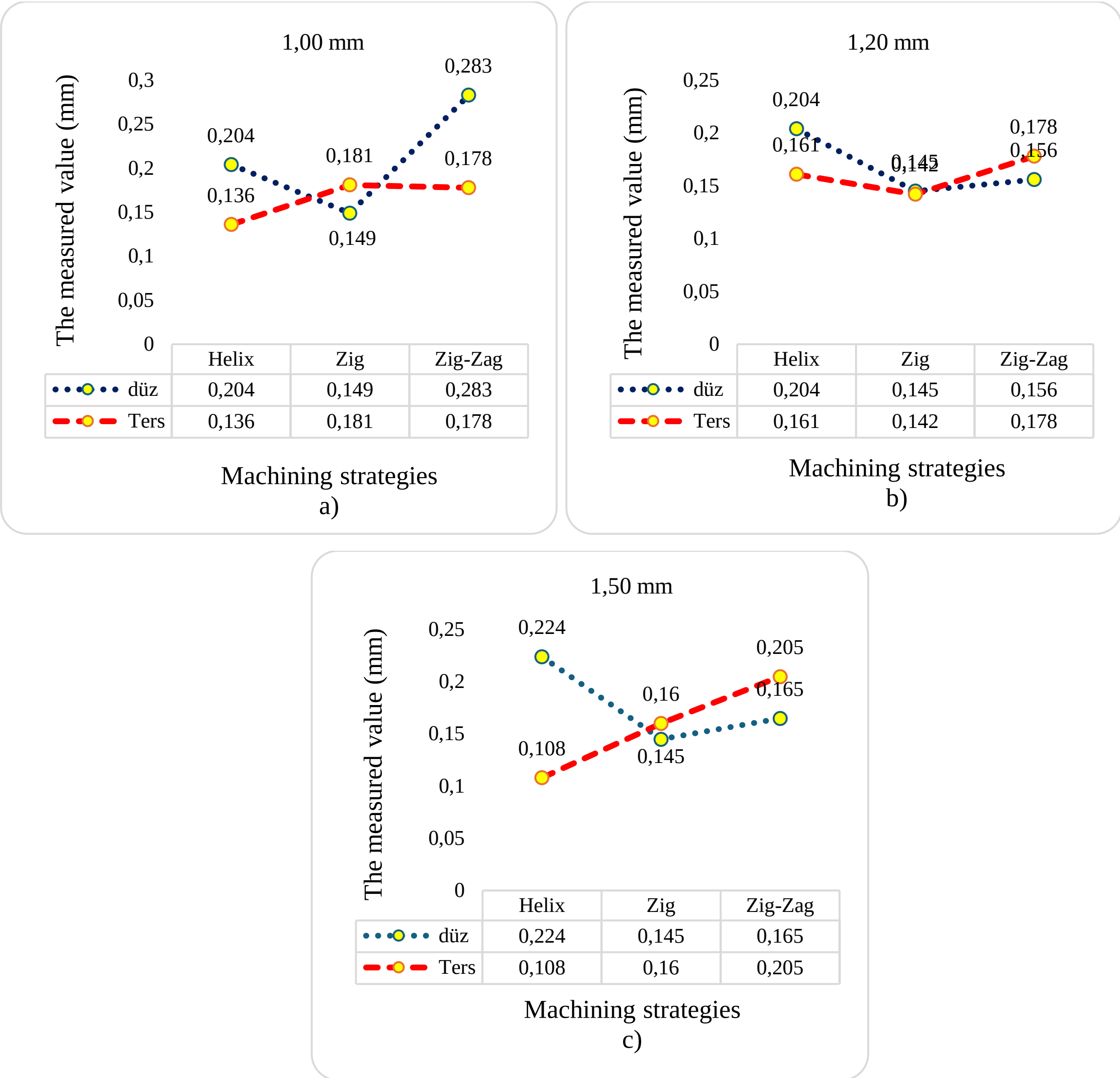

Figure 7. Ra surface roughness measurement -µm (a) 1.00 mm (b) 1.20 mm (c) 1.50 mm

When considering the values where the difference between minimum and maximum surface roughness is minimized, it is observed that zig machining strategy is the least level for all three materials. On the other hand, when considering the values where the difference between minimum and maximum surface roughness is maximized, zig-zag machining is the highest level for the 1.00 mm material, while helix machining is the highest level for the 1.20 mm and 1.50 mm thickness materials. When averaging the minimum and maximum values of the three samples, the average effect value of the machining strategy on surface roughness is found to be 55.46%. This value is consistent with the findings of Ballıkaya (2022), who showed that the tool path shape is the most effective parameter on surface roughness with an effect value of 43.755%. Additionally, the zig-zag tool path shape was found to be the most suitable level. Similarly, in the study conducted by Uzun et al. (2022), they demonstrated that the trochoidal tool strategy is the most ideal machining method for the upper surface with a value of 0.86 µm. Here, considering the minimum and maximum surface roughness, the average effect value of the tool path strategy on surface roughness is evaluated to be an average of 132%. Ballıkaya worked on Sleipner cold work tool steel, while Uzun et al. conducted their studies on AISI X210Cr12 steel.

The parts were subjected to CMM measurements including radius, parallelism, perpendicularity between the bottom surface and inner surface, and perpendicularity between the top surface and inner surface.

Radius measurement result graphs are provided for 1.00 mm in Figure 8a, 1.20 mm in Figure 8b, and 1.50 mm in Figure 8c. Accordingly, for the 1.00 mm thickness part, the radius measurement values of 6.133 mm obtained from the helix-straight machining method yielded the best results. This value is closest to the nominal radius of 6.00 mm. The highest deviation was observed in the zig-zag-reverse machining method, with a measurement of 6.716 mm. For the 1.20 mm thickness part, the radius measurement values were measured as 5.98 mm in the helix-straight machining method, which is closest to the nominal radius of 6.00 mm. The highest deviation was measured as 5.931 mm in the helix-reverse machining method. For the 1.50 mm thickness part, the radius measurement values were measured as 5.992 mm in the helix-straight machining method, which is closest to the nominal radius of 6.00 mm. The highest deviation was measured as 6.096 mm in the zig-reverse machining method.

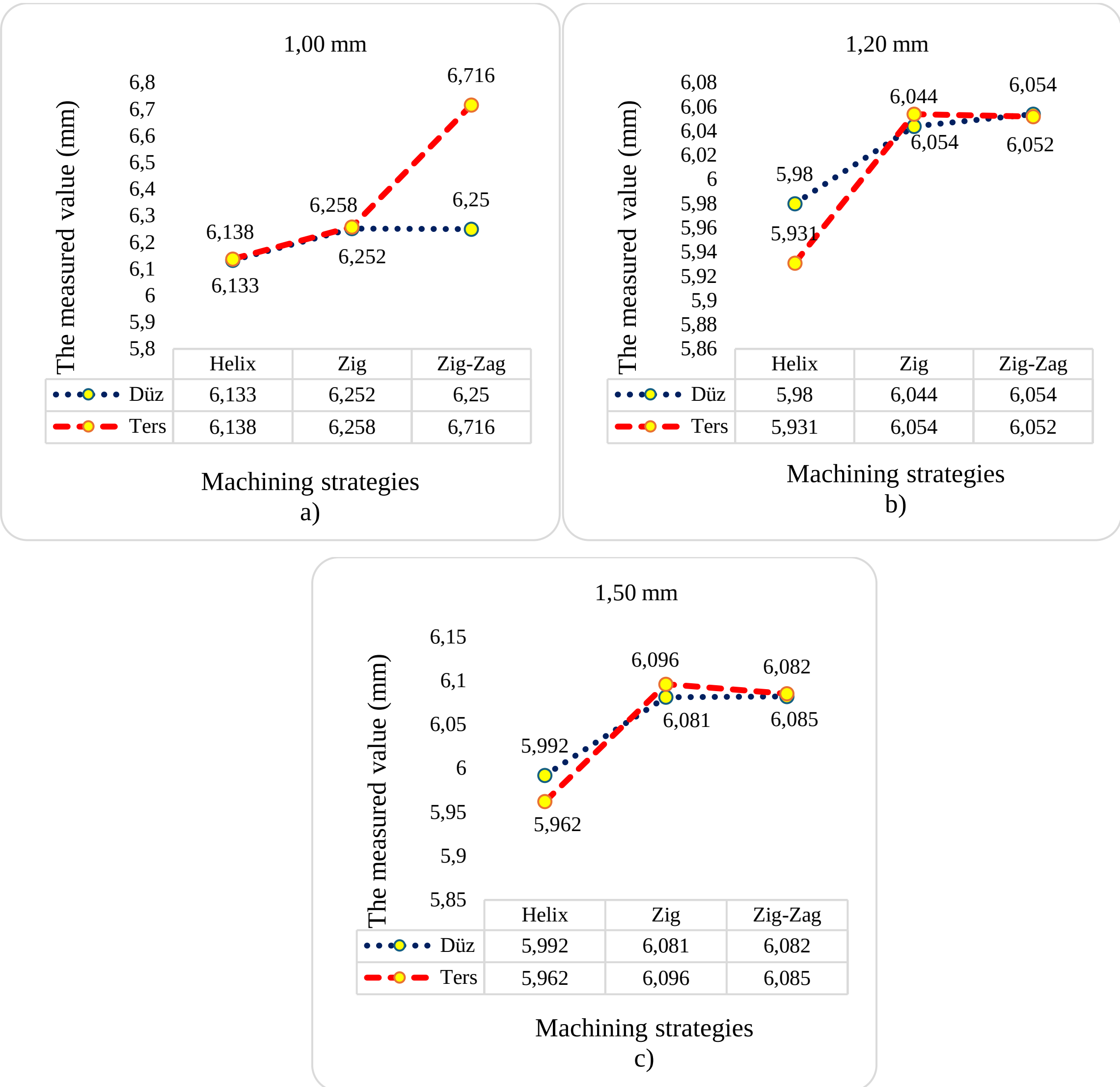

Figure 8. Radius measurement (a) 1.00 mm (b) 1.20 mm (c) 1.50 mm

Parallelism measurement result graphs for the lower and upper surfaces are provided for 1.00 mm in Figure 9a, 1.20 mm in Figure 9b, and 1.50 mm in Figure 9c. Deviation values are measured in millimeters. Accordingly, for the part with a thickness of 1.00 mm, the machining method with the least deviation in parallelism between the lower and upper surfaces was zig-zag-straight machining, with a deviation measurement of 0.004 mm. The method showing the highest deviation was zig-reverse machining, with a value of 0.043 mm. For the part with a thickness of 1.20 mm, the machining method with the least deviation in parallelism between the lower and upper surfaces was zig-straight machining, with a deviation measurement of 0.003 mm. The method showing the highest deviation was zig-reverse machining, with a value of 0.021 mm. For the part with a thickness of 1.50 mm, the machining methods zig-zag-straight and zig-reverse showed a deviation measurement of 0.015 mm in parallelism between the lower and upper surfaces. The method showing the highest deviation was helix-reverse machining, with a value of 0.162 mm.

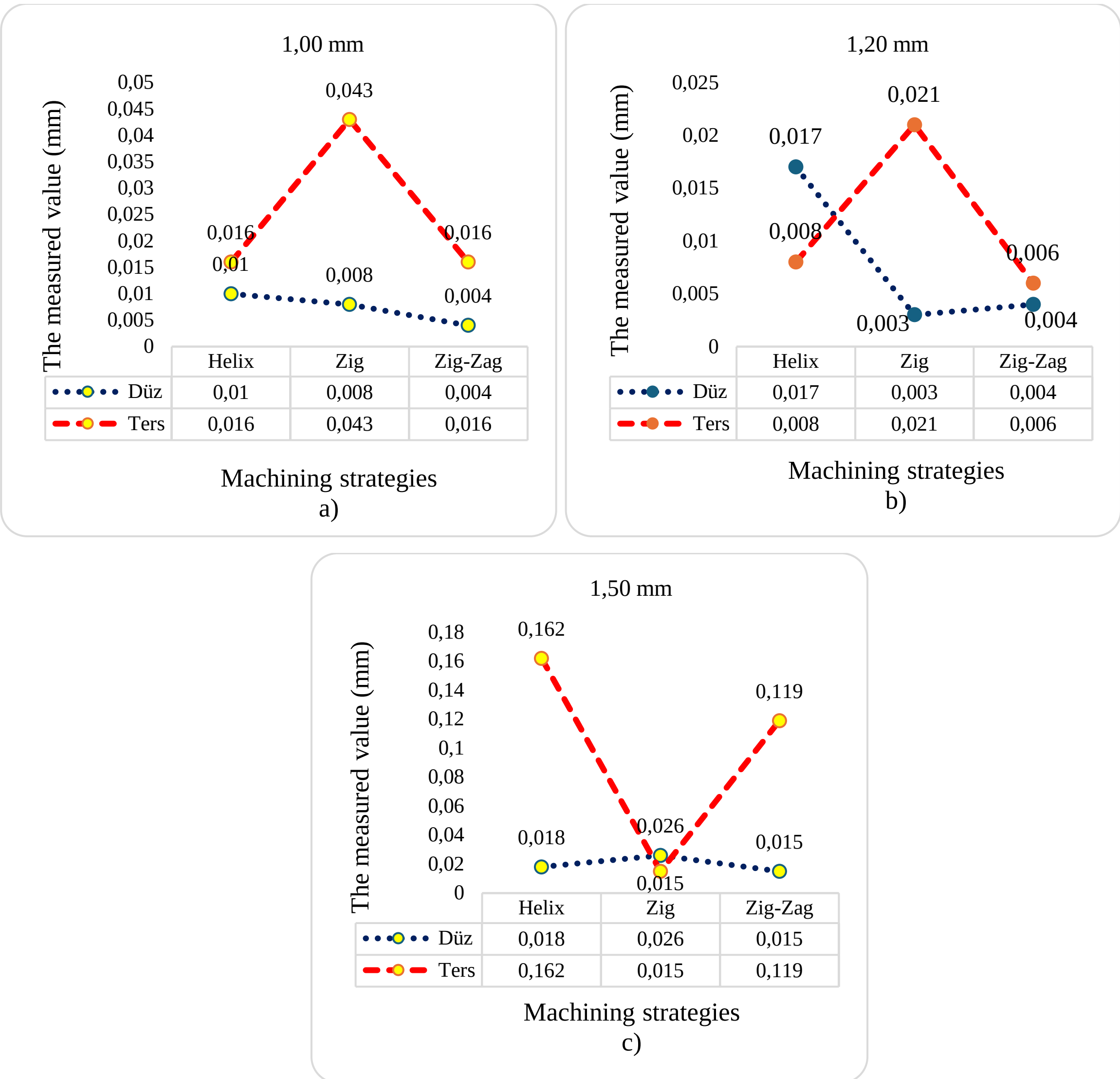

Figure 9. Lower and upper surface parallelism measurement (a) 1.00 mm (b) 1.20 mm (c) 1.50 mm

The graphs of the perpendicularity measurement results between the lower surface and the inner surface are presented for 1.00 mm in Figure 10a, 1.20 mm in Figure 10b, and 1.50 mm in Figure 10c. Deviation values are measured in millimeters. Accordingly, for the part with a thickness of 1.00 mm, the machining methods zig-zag and reverse showed the least deviation in perpendicularity between the lower surface and the inner surface, with a deviation value of 0.001 mm. The method showing the highest deviation was helix-straight machining, with a deviation of 0.035 mm. For the part with a thickness of 1.20 mm, the least deviation in perpendicularity between the lower surface and the inner surface was observed in the zig-zag-straight machining method, with a deviation value of 0.002 mm. The highest deviation was measured in the helix-straight machining method, with a value of 0.029 mm. For the part with a thickness of 1.50 mm, the least deviation in perpendicularity between the lower surface and the inner surface was observed in the zig-reverse machining method, with a value of 0.00 mm. The highest deviation was measured in the helix-straight machining method, with a value of 0.021 mm.

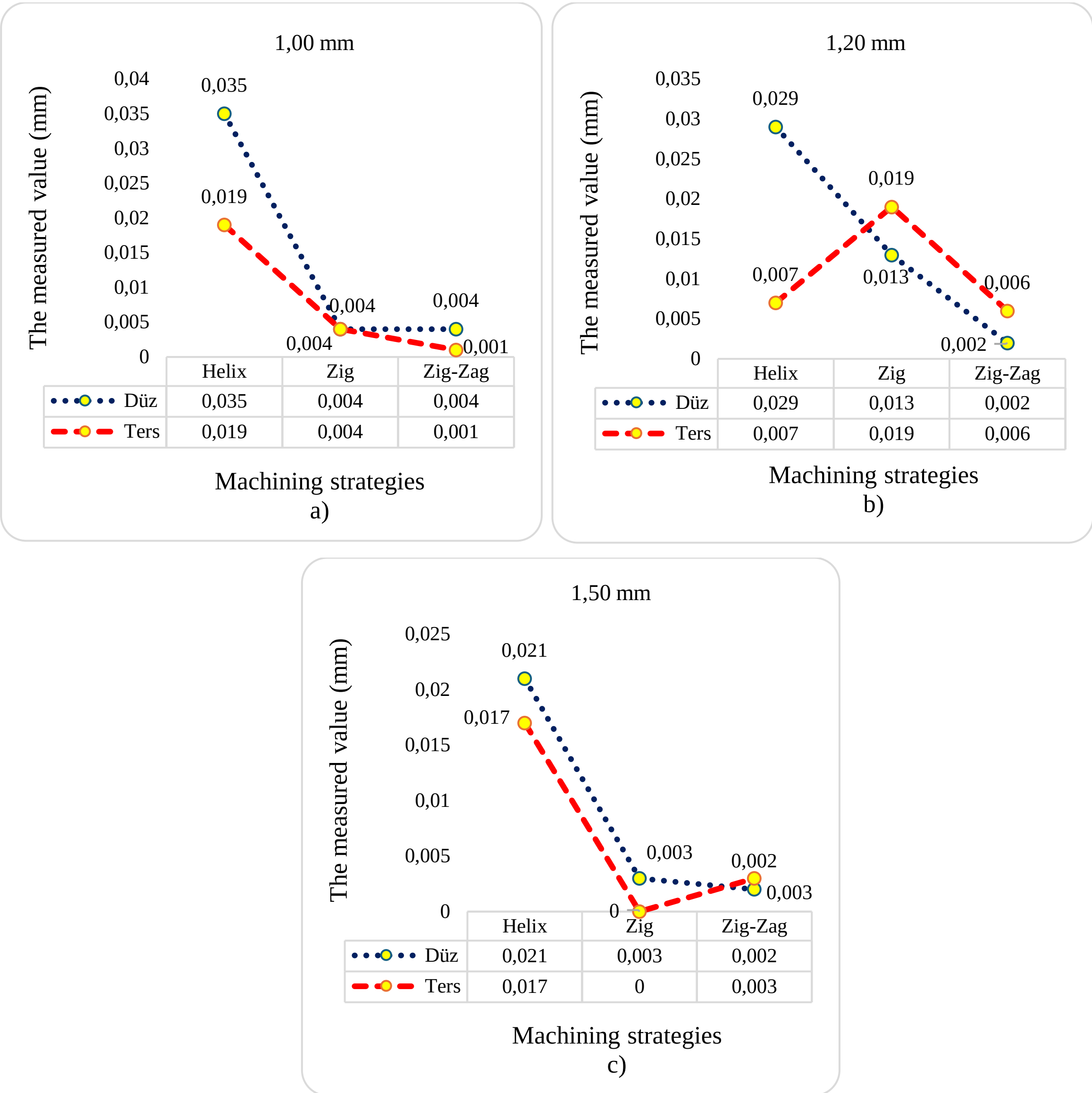

Figure 10. Measurement of clearance between lower surface and inner surface (a) 1.00 mm (b) 1.20 mm (c) 1.50 mm

The graphs of the gap measurement results between the upper surface and the inner surface are provided for 1.00 mm in Figure 11a, 1.20 mm in Figure 11b, and 1.50 mm in Figure 11c. Deviation values are measured in millimeters. Accordingly, for the part with a thickness of 1.00 mm, the least deviation in gap between the upper surface and the inner surface was measured in the zig-reverse machining method, with a deviation of 0.00 mm. The highest deviation was measured in the zig-zag-reverse machining method, with a value of 0.197 mm. For the part with a thickness of 1.20 mm, the deviation in gap between the upper surface and the inner surface was measured. According to these values, the least deviation was measured in the zig-reverse machining method, with a value of 0.00 mm. The highest deviation was measured in the helix-straight machining method, with a value of 0.026 mm. For the part with a thickness of 1.50 mm, the least deviation in gap between the upper surface and the inner surface was measured in the zig-zag-reverse machining method, with a value of 0.006 mm. The highest deviation was measured in the helix-straight machining method, with a value of 0.047 mm.

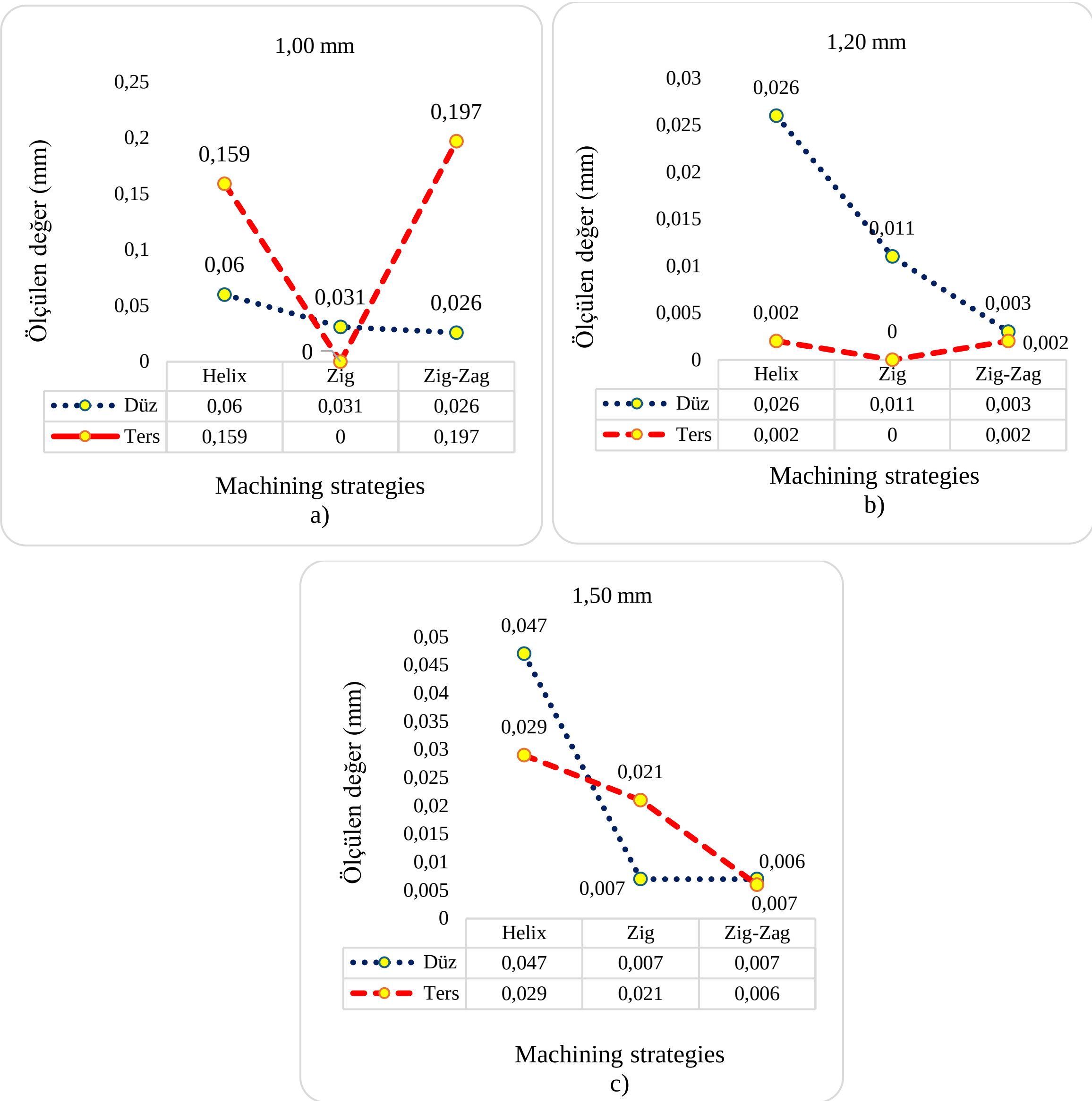

Figure 11. Measurement of clearance between upper surface and inner surface (a) 1.00 mm (b) 1.20 mm (c) 1.50 mm

In the CMM measurements, when evaluating the minimum and maximum values of the parallelism measurements between the bottom and top surfaces of the three samples, it was observed that the variation ranged from a minimum of 37.50% to a maximum of 112.50%. This improvement in values corresponds to a 37% improvement over the initial values, as demonstrated by Iglesias et al. (2024) in their milling path study.

4. CONCLUSION

During machining processes in metalworking, minimizing out-of-tolerance measurements is a critical concern. It is recommended to consider the data obtained in this study to achieve the desired dimensions or values, depending on which type of tolerance is crucial in the region intended for machining according to the part technical drawing. This approach can reduce material waste and lead to obtaining more optimal dimensions and values. The aim of this study is to provide advance information to readers who will process Al 7075 T7351 Aluminum alloy material using different techniques.

In this study, the thickness, surface roughness, and CMM measurements obtained after machining three sample parts with thicknesses of 1.00, 1.20, and 1.50 mm were examined. After machining, a detailed evaluation of the machining methods and strategies was conducted.

1. After machining, thickness measurements of the sample parts were taken according to the tool paths, and their average values were calculated. It was observed that the straight machining method yielded values closer to the desired level compared to the reverse machining method, with values of 0.96, 1.18, and 1.43, respectively. Furthermore, considering the maximum and minimum values across the three experimental samples, it was evaluated that the influence of the machining strategy on thickness ranged from a maximum of 7.78% to a minimum of 0.67%.

2. The measurement results of the sample parts' surface roughness were evaluated. When the averages of all three machining strategies were considered, it was observed that the reverse machining method had lower levels of roughness compared to the straight machining method, with values of 0.165 µm, 0.160 µm, and 0.157 µm, respectively. When considering the maximum difference in surface roughness between the minimum and maximum values of the material, it was observed that the zig-zag tool path was predominant for the 1.00 mm material thickness, while the helix tool path was predominant for the 1.20 mm and 1.50 mm thicknesses. When the average values of the minimum and maximum measurements of the three samples were considered, the average impact of the tool path strategy on surface roughness was found to be 55.46%.

3. The CMM measurements evaluated important parameters such as radius, parallelism, and clearance. When considering the samples closest to the nominal radius values, it was observed that for the 1.00 mm thickness part, the radius measurement values were 6.133 mm for helix-straight machining, for the 1.20 mm thickness part, the radius measurement values were 5.98 mm for helix-straight machining, and for the 1.50 mm thickness part, the radius measurement values were 5.992 mm for helix-straight machining, providing results closest to the nominal radius. In terms of parallelism between the lower and upper surfaces, the minimum deviation values were observed as follows: for the 1.00 mm thickness part, 0.004 mm for zig-zag-straight machining, for the 1.20 mm thickness part, 0.003 mm for zig-straight machining, and for the 1.50 mm thickness part, 0.015 mm for zig-zag-straight machining. Regarding the clearance between the lower surface and the inner surface, the minimum deviation values were observed as follows: for the 1.00 mm thickness part, 0.001 mm for zig-zag-reverse machining, for the 1.20 mm thickness part, 0.002 mm for zig-zag-straight machining, and for the 1.50 mm thickness part, 0.00 mm for zig-reverse machining. In terms of the clearance between the upper

surface and the inner surface, the minimum deviation values were observed as follows: for the 1.00 mm thickness part, 0.00 mm for zig-reverse machining, for the 1.20 mm thickness part, 0.00 mm for zig-reverse machining, and for the 1.50 mm thickness part, 0.006 mm for zig-zag-reverse machining. In the CMM measurements, when the minimum and maximum values of parallelism between the upper and lower surfaces were evaluated for three samples, it was observed that the deviation ranged from a minimum of 37.50% to a maximum of 112.50%. This improvement was shown to be 37% in the study conducted by Iglesias et al. in terms of milling path compared to the initial values.

The results of this study can provide guidance in the selection of machining strategies and methods in industrial production processes. However, for a more comprehensive evaluation of machining strategies and methods, further experiments are necessary. In the future, it is recommended to conduct comprehensive research considering different machining strategies and the effects of cutting parameters for Al 7075 material. Additionally, future work should aim to explore distortion control in the machining of different materials by working with a wide range of material thicknesses and optimizing machining parameters.

REFERENCES

Aggogeri, F., Barbato, G., Barini, E. M., Genta, G., Levi, R. (2011). Measurement uncertainty assessment of Coordinate Measuring Machines by simulation and planned experimentation, CIRP Journal of Manufacturing Science and Technology, 4(1), 51-56. https://doi.org/10.1016/j.cirpj.2011.01.007

Anselmetti, B. (2006). Generation of Functional Tolerancing Based on Positioning Features. Comput. Des. 38, 902–919. DOI:10.1016/j.cad.2006.05.005

Anselmetti, B.; Louati, H. (2005). Generation of Manufacturing Tolerancing with ISO Standards. Int. J. Mach. Tools Manuf. 45, 1124–1131. DOI:10.1016/j.ijmachtools.2005.01.001

Arslan, H., Onmaz, F., Orhan, S. (2024). 7075 Alüminyum Malzemenin Çift Milli Freze ile İşlenmesi Sırasında En Uygun Kesici Parametrelerinin Belirlenmesi. International Journal of Engineering Research and Development, 16(1), 117-126. https://doi.org/10.29137/umagd.1372959

Ballıkaya, H. (2022). Sleipner Soğuk İş Takım Çeliğinin Yüzey Finish Modellemesinde Takım Yolu Stratejisinin ve Kesme Parametrelerinin MRR ve Ra Üzerine Etkisi", DÜMF MD, 13 (1), 35–42. doi: 10.24012/dumf.1051243

Ballu, A. Falgarone, H. Chevassus, N. Mathieu, L. (2006). A New Design Method Based on Functions and Tolerance Specifications for Product Modelling. CIRP Ann. 2006, 55, 139–142. DOI:10.1016/S0007-8506(07)60384-9

Balsamo, A. (2023). Riunione della ISO/TC213 Dimensional and Geometrical Product Specification and Verification / - In: PROBING. 30, 18-28.

Bozdemir, M., Akdeniz, E., Yılmaz, M., Gezer, M. K. (2023). Investigation of the effect of cutting parameters and tool holder on surface roughness and machining precision in al 7075-T6 milling operation," Gazi Journal of Engineering Sciences, vol. 9, no. 3, pp. 535-543, doi:10.30855/gmbd.0705085

Cao, Y., Zhang, H., Li, B., Wu, Z., Yang, J. (2013). Study on Functional Specification Scheme on Interface Based on Positioning Features. Proc. Inst. Mech. Eng. Part B J. Eng. Manuf. 2013, 227, 745–753.

Cauchick-Miguel, P., King, T. Davis, J. (1996). CMM verification: a survey. Measurement, 17 (1), 1-16. https://doi.org/10.1016/0263-2241(96)00001-2

Franco, P., Jodar, J. (2021). Theoretical analysis of straightness errors in coordinate measuring machines (CMM) with three linear axes. International Journal of Precision Engineering and Manufacturing, 22, 63–72. https://doi.org/10.1007/s12541-019-00264-0

Gameros, A., Lowth, S., Axinte, D., Nagy-Sochacki, A., Craig, O., Siller, H. R. (2017). State-of-the-art in fixture systems for the manufacture and assembly of rigid components: A review. International Journal of Machine Tools and Manufacture, 123, 1-21. DOI:10.1016/j.ijmachtools.2017.07.004

Göhler, S.M., Husung, S., Howard, T.J. (2016). The Translation between Functional Requirements and Design Parameters for Robust Design. Procedia CIRP 2016, 43, 106–111. DOI:10.1016/j.procir.2016.02.028

Göktaş M, Güldaş A, Dilipak H. (2017). Tool Path Generation for Pocket Machining Operations with Island. Gazi University Journal of Science. 30:79–88.

Hu, J., Peng, Y. (2011). Development of a Function Oriented Computer Aided Tolerancing (FOCAT) System. Proc. Inst. Mech. Eng. Part B J. Eng. Manuf., 225, 1189–1203. DOI:10.1177/2041297510393578

Iglesias, I., Sanchez, A., Silva, F. J.G. (2024) Robotic path compensation training method for optimizing face milling operations based on non-contact CMM techniques, Robotics and Computer-Integrated Manufacturing, 85, 102623, https://doi.org/10.1016/j.rcim.2023.102623

Imran, M., Khan, A.R.A. (2019). Characterization of Al-7075 metal matrix composites: a review J. Mater. Res. Technol., 8 (3), 3347-3356. 10.1016/j.jmrt.2017.10.012

Işık, U. (2019). Üç Boyutlu Koordinat Ölçme Cihazı (CMM) ile Optik Tarama Cihazının Performanslarının Karşılaştırılması. Yüksek Lisans Tezi. Karabük: Karabük Üniversitesi, Fen Bilimleri Enstitüsü.

ISO 10360-2. (2009). Parametrical product specifications (GPS)—Acceptance and reverification tests for coordinate measuring machines (CMM)—Part 2: CMMs used for measuring linear dimensions.

Jamaludin, Z., Sudianto, A., Mat Seman, N., Othman, A., Maharof, M., Yahaya, S., & Patwari, A. (2023). Performance Analysis of a Cad/Cam-MATLAB/Simulink Interpreter in Milling Machine Application. Journal of Advanced Manufacturing Technology (JAMT), 17(3). Retrieved from https://jamt.utem.edu.my/jamt/article/view/6591

Khalid, M. Y., Umer, R., Khan, K.A. (2023). Review of recent trends and developments in aluminium 7075 alloy and its metal matrix composites (MMCs) for aircraft applications, Results in Engineering, 20,101372, https://doi.org/10.1016/j.rineng.2023.101372.

Kim, J. A., Lee, J. Y., Kang, C. S., Eom, S. H. (2023). Measurement of Six-Degree-of-Freedom Absolute Postures Using a Phase-Encoded Pattern Target and a Monocular Vision System. International Journal of Precision Engineering and Manufacturing. https://doi.org/10.1007/s12541-023-00814-7

Le, X., Pang, D., Wang, Y., Chen, C., Guan, X. (2024). Surface Reconstruction Using Geometric Features and Machining Process, in IEEE Transactions on Instrumentation and Measurement, 73, 1-10, 5008910. doi: 10.1109/TIM.2024.3353870.

Lee, K. I., Jeon, H. K., Lee, J. C., Yang, S. H. (2022). Use of a virtual polyhedron for interim checking of the volumetric and geometric errors of machine tools. International Journal of

Precision Engineering and Manufacturing, 23(10), 1133–1141. https://doi.org/10.1007/s12541-022-00666-7

Lin, M. X., & Hsieh, T. H. (2023). Geometric error parameterization of a CMM via calibrated hole plate archived utilizing DCC formatting. Appl Sci, 13(10), 6344.

Maltauro, M., Meneghello, R., Concheri, G. (2024). Tolerance Specifications Management Integrated into the Product Development Cycle. Machines.12(2):147. https://doi.org/10.3390/machines12020147

Maltauro, M., Morse, E. (2023). Towards a Definition of “Geometric Verification Specifications” Within the ISO GPS System, Procedia CIRP, 119, 339-344. https://doi.org/10.1016/j.procir.2023.03.101

Motorcu, A. R., Bilge, T. (2018). Laminant Kompozitin Cep Frezelemesinde Yüzey Pürüzlülüğü ve Boyutsal Tamlığın Değerlendirilmesi”, DÜBİTED, 6(1), 79–100. doi: 10.29130/dubited.324440.

Pahk, H. J., Burdekin, M. (1991). Evaluation of the effective parametric errors in coordinate measuring machines using the locus of stylus on the horizontal plane. Proc IMechE Part B: Journal of Engineering Manufacture, 205(2), 123–138. https://doi.org/10.1243/PIME_PROC_1991_205_060_02

Pahk, H., Kim, J. (1995). Application of microcomputer for assessing the probe lobing error and parametric errors of CMMs using commercial ring gauges. The International Journal of Advanced Manufacturing Technology, 10, 208–218. https://doi.org/10.1007/BF01179349

Pandian, V., Kannan, S. (2022). Effect of high entropy particle on aerospace-grade aluminium composite developed through combined mechanical supersonic vibration and squeeze infiltration technique. J. Manuf. Process., 74, 383-399, 10.1016/j.jmapro.2021.12.024

Poyraz, Ö., Yandı, N. (2021). Kompresör ve Türbin Palelerinin Fikstür Tasarımlarının Parametrik Analiz ve Sonlu Eleman Simülasyonları ile İncelenmesi. Avrupa Bilim ve Teknoloji Dergisi (28), 97-105. https://doi.org/10.31590/ejosat.989033

Rouetbi, O., Pierre, L., Anselmetti, B., Denoix, H. (2017). ISO Tolerancing of Hyperstatic Mechanical Systems with Deformation Control; Springer: Berlin, Germany, 991–1000. DOI:10.1007/978-3-319-45781-9_99

Royer, M., Anselmetti, B. (2016). 3D Manufacturing Tolerancing with Analysis Line Method Taking into Account Joining Operations During Manufacturing Process. Procedia CIRP. 43. 88-93. 10.1016/j.procir.2016.02.023.

Sato, O. & Takatsuji, T., Balsamo, A. (2022). Practical experimental design of task-specific uncertainty evaluation for coordinate metrology. 10.1142/9789811242380_0023

Shaheen, A., Nielsen, N. E., Bissacco, G. (2023). A comparison of the performance of tool pre-setting optical systems: On- and off machine tool assessment.

Snigdha, M., Sandeep, S.C., Swathi, G., Suresh, R., & Hanuma, P. (2017). Design of Fixture for the Manufacturing of Compressor Rotor Blade in Aircraft Engine. International Journal of Mechanical Engineering and Technology (IJMET), 8, 1034–1051. http://iaeme.com/Home/journal/IJMET

Sudatham, W., Matsumoto, H., Takahashi, S., Takamasu, K. (2015). Verification of the positioning accuracy of industrial coordinate measuring machine using optical-comb pulsed interferometer with a rough metal ball target. Precision Engineering, 41, 63–67. https://doi.org/10.1016/j.precisioneng.2015.01.007

Trapet, E., Savio, E., De Chiffre, L. (2004). New advances in traceability of CMMs for almost the entire range of industrial dimensional metrology needs, CIRP Annals, 53(1), 433-438. https://doi.org/10.1016/S0007-8506(07)60733-1.

Umetsu, K., Furutnani, R., Osawa, S., Takatsuji, T., & Kurosawa, T. (2005). Parametric calibration of a coordinate measuring machine using a laser tracking system. Measurement Science & Technology, 16(12), 2466–2472. https://doi.org/10.1088/0957-0233/16/12/010

Uzun, M., Usca, Ü.A., Kuntoğlu, M., Gupta, M. K. (2022). Influence of tool path strategies on machining time, tool wear, and surface roughness during milling of AISI X210Cr12 steel. Int J Adv Manuf Technol 119, 2709–2720. https://doi.org/10.1007/s00170-021-08365-9

Vlaeyen, M., Haitjema, H., Dewulf, W. (2023). Virtual task-specific measurement uncertainty determination for laser scanning, Precision Engineering, 80, 208-228. https://doi.org/10.1016/j.precisioneng.2022.12.008.

Weckenmann, A. (2011). Koordinatenmesstechnik, Hanser, Münih, 12-17.

Wojtyła, M., Rosner, P., Płowucha, W., Balsamo, A., Piccato, A., Forbes, A. B., Savio, E. (2023). Determination of uncertainty of coordinate measurements on the basis of the formula for EL, MPE, Measurement, 222,2023,113635.

Yang, S. H., Lee, K. I. (2022). A dual difference method for identification of the inherent spindle axis parallelism errors of machine tools. International Journal of Precision Engineering and Manufacturing, 23(6), 701–710. https://doi.org/10.1007/s12541-022-00653-y

Zhou, J., Yue, C., Liu, X., Xia, W., Wei, X., Qu, Ji., Liang, S., Wang, L. (2023). Classification of Tool Wear State based on Dual Attention Mechanism Network. Robotics and Computer-Integrated Manufacturing. 83. 1-14. 10.1016/j.rcim.2023.102575

Zhu, L. (2010). Estimation of Uncertainty in Spatial Straightness Measurement According to Next Generation of GPS Standard System, Third International Workshop on Advanced Computational Intelligence, 666-669.